Accepted Manuscript

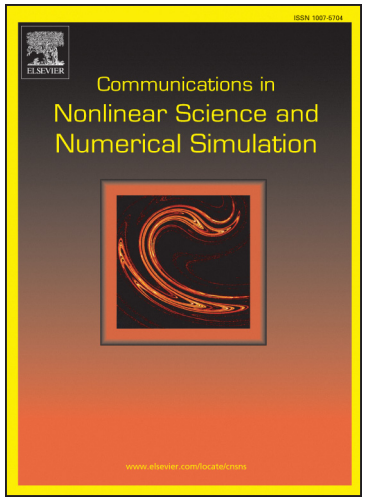

Modelling the regulatory system for diabetes mellitus with a threshold window

Jin Yang, Sanyi Tang, Robert A. Cheke

PII: S1007-5704(14)00395-5
DOI: http://dx.doi.org/10.1016/j.cnsns.2014.08.012
Reference: CNSNS 3311

To appear in: *Communications in Nonlinear Science and Numerical Simulation*

Received Date: 14 January 2014
Revised Date: 3 July 2014
Accepted Date: 16 August 2014

Please cite this article as: Yang, J., Tang, S., Cheke, R.A., Modelling the regulatory system for diabetes mellitus with a threshold window, *Communications in Nonlinear Science and Numerical Simulation* (2014), doi: http://dx.doi.org/10.1016/j.cnsns.2014.08.012

Modelling the regulatory system for diabetes mellitus with a threshold window

Jin Yang[♮], Sanyi Tang[♮] Robert A. Cheke[♯]

♮ *College of Mathematics and Information Science*
Shaanxi Normal University, Xi'an, 710062, P.R. China
Sanyitang219@hotmail.com, sytang@snnu.edu.cn, Tel: +86 29 85310232

♯ *Natural Resources Institute, University of Greenwich at Medway,Central Avenue, Chatham Maritime, Chatham, Kent, ME4 4TB, UK r.a.cheke@greenwich.ac.uk*

Abstract

Piecewise (or non-smooth) glucose-insulin models with threshold windows for type 1 and type 2 diabetes mellitus are proposed and analyzed with a view to improving understanding of the glucose-insulin regulatory system. For glucose-insulin models with a single threshold, the existence and stability of regular, virtual, pseudo-equilibria and tangent points are addressed. Then the relations between regular equilibria and a pseudo-equilibrium are studied. Furthermore, the sufficient and necessary conditions for the global stability of regular equilibria and the pseudo-equilibrium are provided by using qualitative analysis techniques of non-smooth Filippov dynamic systems. Sliding bifurcations related to boundary node bifurcations were investigated with theoretical and numerical techniques, and insulin clinical therapies are discussed. For glucose-insulin models with a threshold window, the effects of glucose thresholds or the widths of threshold windows on the durations of insulin therapy and glucose infusion were addressed. The duration of the effects of an insulin injection is sensitive to the variation of thresholds. Our results indicate that blood glucose level can be maintained within a normal range using piecewise glucose-insulin models with a single threshold or a threshold window. Moreover, our findings suggest that it is critical to individualize insulin therapy for each patient separately, based on initial blood glucose levels.

Keywords: Glucose-insulin model, Insulin therapy, Sliding bifurcation,

Duration, Blood glucose level

1. Introduction

Diabetes mellitus is an epidemic disease worldwide, characterized by plasma glucose concentrations mostly remaining above the normal range. Depending on the pathogenic mechanisms involved, diabetes is classified into two main categories: type 1 and type 2 diabetes. Type 1 diabetes is generally due to the immune system of the patients destroying β cells in the islets of Langerhans of the pancreas and thus preventing production and secretion of insulin. Type 2 diabetes is mainly due to dysfunction of the glucose-insulin regulatory system [1, 2]. Since the discovery of diabetes, many researchers have attempted to find out how the endocrine metabolic system works [3, 4] and why there are dysfunctions [5] in order to devise effective and efficient therapies to improve the daily life of diabetic patients.

In insulin therapies, the subcutaneous injection of insulin or its analogues by using an insulin pump when needed is a typical treatment. This not only provides a basic treatment for type 1 diabetes [6], but also supplies a viable alternative for type 2 diabetes although the latter can be controlled, or even cured, by life-style changes such as dietary adjustment, physical exercise, stopping smoking and avoiding exposure to second-hand smoke [7, 8, 9]. Due to technological difficulties, the main obstacle in insulin therapies, however, is difficulty in the monitoring of plasma glucose concentrations non-invasively. Thus, all current therapies are open-loop treatments that are unable to use the feedback of glucose concentration automatically [10]. When an accurate non-invasive glucose monitoring technique is developed, the open-loop treatment could be replaced by closed-loop therapy, with an artificial pancreas delivering insulin automatically according to variations in blood glucose levels [10, 11, 12].

An artificial pancreas, which is still being developed would function like a real and healthy pancreas allowing diabetic patients to control their blood glucose levels within a normal range automatically [13]. With the help of such an artificial pancreas, patients could improve their life-styles without injecting insulin manually or measuring the glucose infusion rate. However, there are two major impediments to the development of an artificial pancreas including the need for reliable predictive models and the lack of effective and efficient control algorithms [12, 13]. To overcome these problems, several reliable mathematical models of delay differential equations which can de-

termine the time and the dose of insulin injections for control algorithms have been proposed and investigated [14, 15, 16]. Moreover, pulsatile insulin secretion has been employed to mimic impulsive injections for type 1 or type 2 diabetes mellitus treatment regimes [15, 16]. Recently, Huang et al. devised a new mathematical model with open-loop control considering impulsive injection of insulin either periodically or by monitoring the plasma glucose concentration level [13]. The model can be described by

$$\begin{cases} \left.\begin{aligned} &\frac{dG(t)}{dt} = G_{in} - \sigma_2 G(t) - a\left(c + \frac{mI(t)}{n + I(t)}\right) G(t) + b, \\ &\frac{dI(t)}{dt} = \frac{\sigma_1 G^2(t)}{\alpha_1^2 + G^2(t)} - dI(t), \end{aligned}\right\} t \neq h\tau, \\ \left.\begin{aligned} &G(t^+) = G(t), \\ &I(t^+) = I(t) + \sigma, \end{aligned}\right\} \quad t = h\tau, \end{cases} \tag{1.1}$$

where $G(t)$ is the glucose concentration at time t, $I(t)$ is the insulin concentration at time t, G_{in} is the estimated average constant rate of glucose input, σ_2 indicates the insulin-independent glucose uptake rate, the term $aG(t)(c + mI(t)/(n + I(t)))$ stands for the insulin-dependent glucose utilization, b represents the hepatic glucose production, $\sigma_1 G^2(t)/(\alpha_1^2 + G^2(t))$ is insulin secretion stimulated by elevated glucose concentration caused by complex pathways including chemical-electrical processes, d indicates the insulin degradation rate. In addition, all parameters are positive (for details see [13]), with initial condition $G(0) = G_0 > 0, I(0) = I_0 > 0$. τ is the period of the impulsive injection of insulin, σ denotes the dose of insulin in each injection applied as an impulse at discrete times $t = h\tau, h \in Z^+ = \{1, 2, 3, ...\}$.

Note that insulin pumps with an open-loop approach have made significant contributions to insulin clinical therapies. However, open-loop therapy changes the life-styles of the patients and increases their likelihoods of becoming hyperinsulinaemic or hyperglycaemic. For example, a patient has to inject insulin at a fixed time without monitoring the plasma glucose concentrations automatically. So the following questions arise: what is an ideal treatment for diabetes patients and how does it work? From both practical and theoretical points of view, the most effective insulin therapy for diabetes patients is to control their blood glucose levels within a desirable range, once the blood glucose reaches a critical glucose threshold (CGT) instead of periodic injections of insulin. Meanwhile, when the blood glucose level is below the critical glucose threshold, diabetes patients can take up glucose normally,

as shown in Fig. 1.

The critical glucose threshold can be defined as the glucose level in the blood when insulin injections must be taken to prevent the dangerous glucose level (DGL) from being reached and exceeded, where the DGL is the blood glucose level that will cause harm to patients. For example, insulin injections must be taken once the critical concentration of glucose is observed by a glucose monitoring system so that the DGL cannot be exceeded, i.e., sufficient lead time is needed between the time when the critical concentration of glucose is observed and the time when a treatment is applied (obviously, CGT is less than DGL). Then it is revealed that the most reasonable treatment is when insulin is injected automatically in a closed-loop technique integrated with the glucose monitoring system.

A blood glucose level within the normal range is needed for human body organs to play their roles in maintaining relevant biological activities. Otherwise, hyperglycaemia induces glucotoxicity, while hypoglycaemia suppresses normal functioning of the organs [17]. For these reasons, the patients must initiate insulin therapy once the blood glucose level has climbed above an upper threshold (denoted by G^{TH}, $G^{TH} \leq 120mg/dl$) and suspend it once the blood glucose level dips below a lower threshold (denoted by G_{TH}, $G_{TH} \geq 60mg/dl$), where $[G_{TH}, G^{TH}]$ is called a threshold window of treatment decision [18]. In this case, we can extend model (1.1) by replacing the impulsive injection of insulin by lower and upper thresholds, which can be written as the following two states.

Glucose infusion state

$$\begin{cases} \dfrac{dG(t)}{dt} = G_{in} - \sigma_2 G(t) - a\left(c + \dfrac{mI(t)}{n + I(t)}\right) G(t) + b, \\ \dfrac{dI(t)}{dt} = \dfrac{\sigma_1 G^2(t)}{\alpha_1^2 + G^2(t)} - dI(t), \end{cases} \quad \text{until} \quad G \downarrow G_{TH}. \tag{1.2}$$

Insulin injection state

$$\begin{cases} \dfrac{dG(t)}{dt} = b - \sigma_2 G(t) - a\left(c + \dfrac{mI(t)}{n + I(t)}\right) G(t), \\ \dfrac{dI(t)}{dt} = \dfrac{\sigma_1 G^2(t)}{\alpha_1^2 + G^2(t)} - dI(t) + \sigma, \end{cases} \quad \text{until} \quad G \uparrow G^{TH}. \tag{1.3}$$

Where all parameters are the same as those in model (1.1). For type 1 diabetes, all or most β-cells are dysfunctional and thus no insulin is secreted.

Such a case corresponds to $\sigma_1 = 0$ in models (1.2) and (1.3). For type 2 diabetes, the β-cells of patients cannot produce enough insulin or so-called insulin resistance occurs when the system becomes dysfunctional and prevents cells from taking up glucose efficiently. Such a case corresponds to $\sigma_1 > 0$ in models (1.2) and (1.3). Note that according to models (1.2) and (1.3), for a patient, if $G(t_0) > G^{TH}$, this patient could be in the insulin injection state; if $G(t_0) < G_{TH}$, he/she could be in the glucose infusion state; if $G_{TH} < G(t_0) < G^{TH}$, he/she may either be in the insulin injection state or be in the glucose infusion state, depending on whether the blood glucose is tending to increase or decrease.

Moreover, when the lower threshold G_{TH} is equal to the upper threshold G^{TH} (i.e., $G_{TH} = G^{TH} = G_C$), then this corresponds to a special case for models (1.2) and (1.3) with a single threshold. In this case the models (1.2) and (1.3) can be rewritten as a Filippov system, a model which has been applied widely in many fields of science and engineering. Furthermore, the theory of Filippov systems is being recognized as not only richer than the corresponding theory of continuous systems, but also as representing a more natural framework for the mathematical modelling of real-world phenomena [18-29].

The paper is arranged as follows. In section 2, the global dynamics of models (1.2) and (1.3) with a single threshold are studied in detail: the existence and stability of several types of equilibria are discussed and the relations between the existence of a regular equilibrium and a pseudo-equilibrium are also discussed. Meanwhile, by using qualitative analysis techniques of non-smooth Filippov dynamic systems the sufficient and necessary conditions for the global stability of regular points and a pseudo-equilibrium are provided, and then sliding bifurcations related to boundary node bifurcations are investigated by employing theoretical and numerical techniques. Furthermore, in section 3, using our proposed piecewise dynamic models with a threshold window we will explore the effects of glucose thresholds or the widths of threshold windows on the durations of insulin therapy and glucose infusion processes (i.e., the number of switches between the insulin injection state and the glucose infusion state).

2. Qualitative analysis and biological implications of models with a single threshold

2.1. Qualitative behaviour of models (1.2) and (1.3)

If $G < G_C$, then the qualitative behaviour of system (1.2) is determined by the following subsystem:

$$\begin{cases} \dfrac{dG(t)}{dt} = (G_{in} + b) - \xi G(t) - \dfrac{amI(t)G(t)}{n + I(t)} = P_1(G, I), \\ \dfrac{dI(t)}{dt} = \dfrac{\sigma_1 G^2(t)}{\alpha_1^2 + G^2(t)} - dI(t) = Q_1(G, I), \end{cases} \tag{2.1}$$

where we denote $\xi = \sigma_2 + ac$ throughout the paper. For $\sigma_1 \geq 0$, there exists an unique positive equilibrium $E_1(G_1, I_1)$ of system (2.1) with $G_1 > 0$ and $I_1 > 0$. The linearized system of (2.1) at the equilibrium $E_1(G_1, I_1)$ is as follows:

$$\begin{cases} \dfrac{dG(t)}{dt} = a_{11}G + a_{12}I, \\ \dfrac{dI(t)}{dt} = a_{21}G + a_{22}I, \end{cases}$$

where $a_{11} = -\xi - amI_1/(n+I_1)$, $a_{12} = -amnG_1/(n+I_1)^2$, $a_{21} = 2\alpha_1^2\sigma_1 G_1/(\alpha_1^2 + G_1^2)^2$, $a_{22} = -d$. Let $p = -(a_{11} + a_{22})$, $q = a_{11}a_{22} - a_{12}a_{21}$, $p > 0$ and $q > 0$ hold true provided that $G_1 > 0$ and $I_1 > 0$. Denote $\Delta_1 = p^2 - 4q$, when $\Delta_1 \geq 0$, E_1 is a stable node, and when $\Delta_1 < 0$, E_1 is a stable focus. Choosing Dulac function $B(G, I) = 1$, then we have

$$\frac{\partial BP_1}{\partial G} + \frac{\partial BQ_1}{\partial I} = -\xi - \frac{amI}{n + I} - d < 0.$$

Therefore, according to the Bendixson theorem, no closed orbit for system (2.1) exists, which implies that E_1 is globally asymptotically stable.

If $G > G_C$, the qualitative behaviour of system (1.3) is guaranteed by the following subsystem

$$\begin{cases} \dfrac{dG(t)}{dt} = b - \xi G(t) - \dfrac{amI(t)G(t)}{n + I(t)}, \\ \dfrac{dI(t)}{dt} = \dfrac{\sigma_1 G^2(t)}{\alpha_1^2 + G^2(t)} - dI(t) + \sigma, \end{cases} \tag{2.2}$$

Similarly, there exists an unique equilibrium $E_2(G_2, I_2)$ of system (2.2) with $G_2 > 0$ and $I_2 > 0$, and E_2 is globally asymptotically stable.

Lemma 2.1. E_1 of system (2.1) and E_2 of system (2.2) are both globally asymptotically stable.

2.2. Existence of sliding segment

Let

$$\begin{aligned} F_{S_1}(Z) &= \left((G_{in}+b)-\xi G(t)-\tfrac{amI(t)G(t)}{n+I(t)}, \tfrac{\sigma_1 G^2(t)}{\alpha_1^2+G^2(t)}-dI(t)\right)^T \\ &\doteq (f_1(G,I), g_1(G,I))^T, \\ F_{S_2}(Z) &= \left(b-\xi G(t)-\tfrac{amI(t)G(t)}{n+I(t)}, \tfrac{\sigma_1 G^2(t)}{\alpha_1^2+G^2(t)}-dI(t)+\sigma\right)^T \\ &\doteq (f_2(G,I), g_2(G,I))^T. \end{aligned}$$

then systems (1.2) and (1.3) can be written as the following Filippov system [30]

$$\dot{Z}(t) = \begin{cases} \frac{dZ(t)}{dt} = F_{S_1}(Z), & Z \in S_1, \\ \frac{dZ(t)}{dt} = F_{S_2}(Z), & Z \in S_2, \end{cases} \tag{2.3}$$

where

$$S_1 = \{Z \in R_+^2 | H(Z) < 0\}, S_2 = \{Z \in R_+^2 | H(Z) > 0\}$$

with $H(Z) = G - G_C$ and $R_+^2 = \{Z = (G, I)^T | G \geq 0, I \geq 0\}$.

Furthermore, the discontinuity boundary (or manifold) Σ separating the two regions S_1 and S_2 is described as $\Sigma = \{Z \in R_+^2 | H(Z) = 0\}$. From now on, we call Filippov system (2.3) defined in region S_1 and S_2 as system S_1 and S_2, respectively.

Let

$$\sigma(Z) = \langle H_Z(Z), F_{S_1}(Z)\rangle \langle H_Z(Z), F_{S_2}(Z)\rangle,$$

where $\langle\cdot\rangle$ denotes the standard scalar product. Then the interior of the sliding mode domain can be defined as [26, 31, 32]

$$\Sigma_S = \{Z \in \Sigma | \sigma(Z) < 0\}.$$

According to the definition of $\sigma(Z)$, we have

$$\sigma(Z) = \left\{(G_{in}+b) - \xi G_C - \frac{amIG_C}{n+I}\right\} \cdot \left\{b - \xi G_C - \frac{amIG_C}{n+I}\right\},$$

solving the inequality $\sigma(Z) < 0$ yields

$$I_{c2} \doteq \frac{n(b-\xi G_C)}{(am+\xi)G_C - b} < I < \frac{n(G_{in}+b-\xi G_C)}{(am+\xi)G_C - G_{in} - b} \doteq I_{c1}.$$

Therefore, the sliding segment of Filippov system (2.3) can be defined as

$$\Sigma_S = \{(G,I)^T \in R_+^2 | G = G_C, \max\{I_{c2}, 0\} < I < I_{c1}\}.$$

2.3. Sliding mode dynamics and existence of the equilibria

The following definitions of all types of equilibria of Filippov system (2.3) are necessary throughout the paper [19, 26, 31, 32].

Definition 2.1. A point Z^* is called a regular equilibrium of system (2.3) if $F_{S_1}(Z^*) = 0$, $H(Z^*) < 0$ or $F_{S_2}(Z^*) = 0$, $H(Z^*) > 0$. A point Z^* is called a virtual equilibrium of system (2.3) if $F_{S_1}(Z^*) = 0$, $H(Z^*) > 0$ or $F_{S_2}(Z^*) = 0$, $H(Z^*) < 0$.

Definition 2.2. A point Z^* is called a pseudo-equilibrium if it is an equilibrium of the sliding mode of system (2.3), i.e. $\lambda F_{S_1}(Z^*) + (1-\lambda)F_{S_2}(Z^*) = 0$ and $0 < \lambda < 1$, where

$$\lambda = \frac{\langle H_Z(Z), F_{S_2}(Z)\rangle}{\langle H_Z(Z), F_{S_2}(Z) - F_{S_1}(Z)\rangle}.$$

Definition 2.3. A point Z^* is called a boundary equilibrium of system (2.3) if $F_{S_1}(Z^*) = 0$, $H(Z^*) = 0$ or $F_{S_2}(Z^*) = 0$, $H(Z^*) = 0$.

Definition 2.4. A point Z^* is called a tangent point of system (2.3) if $Z^* \in \Sigma_S, F_S(Z^*) \neq 0$ and $[F_{S_1} \cdot H(Z^*)][F_{S_2} \cdot H(Z^*)] = 0$. Moreover, Z^* is a visible (invisible) tangent point of F_{S_1} if $F_{S_1} \cdot H(Z^*) = 0$ and $F_{S_1}^2 \cdot H(Z^*) > 0 (F_{S_1}^2 \cdot H(Z^*) < 0)$.

The dynamics on the sliding mode Σ_S can be obtained by using Utkin′s equivalent control method [33], i.e. we have

$$\frac{dI}{dt} = \frac{\sigma_1 G_C^2}{\alpha_1^2 + G_C^2} - dI + \sigma\left(\frac{G_{in} + b - \xi G_C - \frac{amIG_C}{n+I}}{G_{in}}\right) = \phi(I).$$

There may be four types of equilibria for Filippov system (2.3): regular equilibrium (denoted as E_R), virtual equilibrium (denoted as E_V), pseudo-equilibrium (denoted as E_P) and boundary equilibrium (denoted as E_B),

while the tangent point is denoted as E_T. From the analysis of section 2.1, we have the following results.

We can see that $G_1 > G_2$ must hold. Let I_1 and I_2 be an arbitrarily constant I_d, and substitute it into the first equation of models (2.1) and (2.2), thus $G_1 = (G_{in} + b)(n + I_d)/((am + \xi)I_d + n\xi) > b(n + I_d)/((am + \xi)I_d + n\xi) = G_2$. Therefore, if $0 < G_C < G_2$, then E_1 becomes a virtual equilibrium denoted by E_V^1 and E_2 is a regular equilibrium denoted by E_R^2. If $G_2 < G_C < G_1$, then E_1 and E_2 are both virtual equilibria. If $G_C > G_1$, then E_1 is a regular equilibrium denoted by E_R^1 and E_2 becomes a virtual equilibrium denoted by E_V^2.

Now we investigate the pseudo-equilibrium of the system (2.3). Solving $\phi(I) = 0$, we get the following equation

$$dG_{in}I^2 + AI - B = 0,$$

where $A = dnG_{in} + \sigma amG_C - (\sigma_1 G_C^2 G_{in}/(\alpha_1^2 + G_C^2) + \sigma(G_{in} + b - \xi G_C))$ and $B = n\left(\sigma_1 G_C^2 G_{in}/(\alpha_1^2 + G_C^2) + \sigma(G_{in} + b - \xi G_C)\right)$. Denote $\Delta = A^2 + 4dG_{in}B$, we get a unique positive root denoted by $I_P = (-A + \sqrt{\Delta})/2dG_{in}$.

Therefore, there is an unique positive pseudo-equilibrium $E_P = (G_C, I_P)$ provided that $I_P \in \Sigma_S$.

The tangent points of Σ_S satisfy $G = G_C$ and

$$G_{in} - \xi G_C - \frac{amI(t)G_C}{n + I(t)} + b = 0, \quad b - \xi G_C - \frac{amI(t)G_C}{n + I(t)} = 0.$$

Then there are two tangent points denoted as $E_T^1 = (G_C, I_{c1})$ and $E_T^2 = (G_C, I_{c2})$ for subsystem S_1 and S_2, respectively.

The boundary equilibrium of Filippov system (2.3) satisfies $G = G_C$, equations (2.1) and (2.2), then the boundary equilibrium of system (2.3) is obtained as follows

$$E_B^1 = \left(G_C, \frac{\sigma_1 G_C^2}{d(\alpha_1^2 + G_C^2)}\right), \text{or } E_B^1 = \left(G_C, \frac{\sigma_1 G_C^2}{d(\alpha_1^2 + G_C^2)} + \frac{\sigma}{d}\right).$$

Lemma 2.2. The two virtual equilibria E_V^1 and E_V^2, and the pseudo-equilibrium E_P can coexist in Filippov system (2.3). Further, the pseudo-equilibrium E_P is stable in the sliding domain Σ_S.

Proof. When $I_P \in (I_{c2}, I_{c1})$, i.e.

$$I_{c2} < \frac{-A + \sqrt{\Delta}}{2dG_{in}} < I_{c1},$$

where $I_{c1} = n(G_{in} + b - \xi G_C)/((am + \xi)G_C - G_{in} - b)$ and $I_{c2} = n(b - \xi G_C)/((am + \xi)G_C - b)$. By direct calculation, we get $G_2 < G_C < G_1$. This inequality is equivalent to the conditions for the coexistence of two virtual equilibria E_V^1 and E_V^2.

In order to prove that E_P is stable in the sliding domain, we only need to prove that the inequality $\phi'(I_P) < 0$. By simple calculation we get

$$\phi'(I_P) = -d - \frac{\sigma amnG_C}{G_{in}(n + I_P)^2} < 0,$$

therefore, E_P is stable. The proof is complete.

Now we investigate the global dynamic behaviour of the Filippov system (2.3).

2.4. Global qualitative analysis of Filippov system (2.3)

Based on the subsection 2.3, E_T^1 is a tangent point of subsystem S_1, E_T^2 is a tangent point of subsystem S_2. Further, E_T^1 is visible provided that $G_C \neq G_1$ and $G_C > G_1$, E_T^1 is invisible provided that $G_C \neq G_1$ and $G_C < G_1$. E_T^2 is visible provided that $G_C \neq G_2$ and $G_C < G_2$; E_T^2 is invisible provided that $G_C \neq G_2$ and $G_2 < G_C$. Then we can get the following theorems.

Theorem 2.3. The equilibrium E_2 of Filippov system (2.3) is globally asymptotically stable if and only if $0 \leq G_C < G_2$.

Theorem 2.4. There exists a globally asymptotically stable pseudo-equilibrium E_P in Filippov system (2.3) if and only if $G_2 \leq G_C \leq G_1$.

Theorem 2.5. The equilibrium E_1 of Filippov system (2.3) is globally asymptotically stable if and only if $G_C > G_1$.

The proofs of Theorems 2.3, 2.4 and 2.5 are provided in Appendix A, Appendix B and Appendix C, respectively.

Remark. Based on the above analyses, it is known that for the Filippov system (2.3) there exist globally asymptotically stable equilibria E_1 or E_2 or a pseudo-equilibrium E_P under certain conditions. From a biological viewpoint, it indicates that with different values of the threshold the blood glucose and the insulin concentrations may stabilize at different fixed levels represented by E_1, E_2 and E_P. This suggests that the threshold G_C can be selected as a basis to control the blood glucose concentration at a desired level within the normal range.

Note that the main results would play a key role in determining the threshold conditions, which guarantee that the blood glucose level is maintained within a normal range. In the coming section, we will investigate the bifurcation analysis and biological implications of model (2.3) for type 2 diabetes, both theoretically and numerically.

2.5. Bifurcation analysis and biological implications of Filippov system (2.3) for type 2 diabetes

In insulin therapies, the use of an insulin pump provides the basic treatment for diabetes [7, 8, 9]. In section 2.4, the dynamical behaviour of Filippov system (2.3) has been investigated in detail. In this section, we address the biological implications of our main results by using bifurcation analysis.

The parameter values for models (1.2) and (1.3) (provided in Table 1) used in our simulations were either determined by previous research [3, 4, 13, 34, 35], or obtained from models for the intravenous glucose tolerance test (IVGTT) [35-37]. We converted units as appropriate and adjusted the values to be within reasonable ranges.

Firstly, the bifurcation set of equilibria and sliding mode will be investigated. We address the richness of the possible equilibria and sliding modes that Filippov system (2.3) can exhibit; we chose parameters b and G_C to build the bifurcation diagram and fixed all other parameters as those in Table 1. Then we can define lines for parameters b and G_C as follows: $L_1 = \{(G_C, b)|b = G_C((am + \xi)I_1 + \xi n)/(n + I_1) - G_{in}\}$, $L_2 = \{(G_C, b)|b = G_C((am + \xi)I_2 + \xi n)/(n + I_2)\}$, where $I_1 = \sigma_1 G_C^2/d(\alpha_1^2 + G_C^2)$ and $I_2 = \sigma_1 G_C^2/d(\alpha_1^2 + G_C^2) + \sigma/d$.

The lines L_1 and L_2 divide G_C and b parameter space into three regions, and the existence or coexistence of regular or virtual equilibria are indicated in each region. Note that the boundary equilibrium E_B^1 (or E_B^2) can exist only on the line L_1 (or L_2) and the existence of sliding modes are indicated in the region between L_1 and L_2. For example, if we fix $b = 50mg/min$, as G_C increases, then E_V^1 and E_R^2 coexist $\rightarrow$ E_B^1 exists $\rightarrow$ E_V^1, E_V^2 and sliding domain Σ_S coexist $\rightarrow$ E_B^1 exists $\rightarrow$ E_R^1 and E_V^2 coexist (for details see Fig.2). It is clear that bifurcations can occur when one of the parameters, such as G_C, varies, which we will address in more detail below.

A boundary node bifurcation for system (2.3) may occur once the equilibria E_R^2, E_T^2 and E_B^2 collide together simultaneously when G_C passes through

a critical value [19, 26]. Choosing the parameter $G_C = 39.18mg/dl$, then the regular equilibrium E_R^2, the visible tangent point E_T^2 and the boundary equilibrium E_B^2 can collide together at E_B^2, as shown in Fig.3(b), where G_C can be obtained by $G_C = b(n+I_2)/((am+\xi)I_2+\xi n)$, and this boundary equilibrium E_B^2 is an attractor with an incoming stable sliding orbit. This implies that the blood glucose and the insulin concentration can stabilize at a fixed level (i.e. E_B^2). When G_C satisfies $0 < G_C < b(n+I_2)/((am+\xi)I_2+\xi n)$, then E_1 becomes a virtual equilibrium and E_2 is a globally stable regular equilibrium. Furthermore, the regular equilibrium E_R^2, the invisible tangent point E_T^1 and the visible tangent point E_T^2 can coexist (see Fig.3(a)). In this case, injection of insulin controls the blood glucose level at a low level (less than $60mg/dl$) leading to hypoglycaemia, which suppresses normal functioning of the body's organs. In addition, E_R^2 and E_T^2 collide at $G_C = b(n+I_2)/((am+\xi)I_2+\xi n)$, and are substituted by a stable pseudo-equilibrium E_P and an invisible tangent point E_T^2 for $b(n+I_2)/((am+\xi)I_2+\xi n) < G_C < (G_{in}+b)(n+I_1)/((am+\xi)I_1+\xi n)$, as shown in Fig.4(a) with $G_C = 100mg/dl$. This means that the blood glucose level stabilizes at the pseudo-equilibrium ($100mg/dl$), which indicates that the blood glucose level could be successfully maintained at a desired level within the normal range. Besides, this bifurcation shows how a stable node becomes a stable pseudo-equilibrium.

Moreover, another boundary node bifurcation for system (2.3) occurs at $G_C = 130.32mg/dl$ (Fig.4), where G_C is obtained by $G_C = (G_{in}+b)(n+I_1)/((am+\xi)I_1+\xi n)$. In this case the boundary equilibrium E_B^1 is stable (Fig.4(b)). The virtual equilibrium E_V^1, the virtual equilibrium E_V^2, the invisible tangent point E_T^1 and E_T^2 and the stable pseudo-equilibrium E_P coexist when $b(n+I_2)/((am+\xi)I_2+\xi n) < G_C < (G_{in}+b)(n+I_1)/((am+\xi)I_1+\xi n)$ with $G_C = 100mg/dl$ (see Fig.4(a)). Further, they collide at $G_C = (G_{in}+b)(n+I_1)/((am+\xi)I_1+\xi n)$. When $G_C > (G_{in}+b)(n+I_1)/((am+\xi)I_1+\xi n)$, there is only a stable regular equilibrium E_R^1 and part of the sliding domain Σ_S, as shown in Fig.4(c). This implies that the patient will be free from insulin therapy, and the blood glucose stabilizes at a high level (large than $120mg/dl$) which leads to hyperglycaemia and glucotoxicity. Therefore, it suggests that the threshold G_C should be carefully chosen by medical workers to maintain the blood glucose level at a desired level. It is manifest that this bifurcation indicates how a stable pseudo-equilibrium becomes a stable node.

From the bifurcation analysis, we can choose the threshold level G_C (for example, $G_C = 100mg/dl$ which belongs to the normal range) such that all

equilibria of each subsystem such as system S_1 and system S_2 become virtual, and the pseudo-equilibrium lying in the sliding mode domain is globally stable. This not only can prevent the possibility of hypoglycaemia and hyperglycaemia, but also constrains the blood glucose level to stabilize at a desired level by insulin therapy. These results clarify that the model (2.3) for type 2 diabetes proposed here can provide reliable predictive outcomes to model the regulatory system for diabetes. Similar results can be obtained for type 1 diabetes (not shown here).

3. Investigations of insulin therapy with a threshold window

The insulin therapy with a single threshold indicates that the blood glucose can be controlled at a desired level within the normal range. Now, we focus on piecewise glucose-insulin systems (1.2) and (1.3) with two threshold values, or with a threshold window, which are proposed for modelling the regulatory system for diabetes. In particular, as discussed in the introduction, insulin therapy with a threshold window allows a patient to continue the injection of insulin until his/her blood glucose level drops down to the lower threshold value G_{TH}, then suspend the therapy; the insulin therapy is only re-started when the blood glucose level goes over the upper threshold value G^{TH}. It would be interesting to investigate how the threshold window governs the durations of insulin therapy and glucose infusion and dynamics of the blood glucose level, in addition to clinical outcomes. We use the proposed models (1.2) and (1.3) for these purposes. In order to avoid redundancy, we mainly focused on type 2 diabetes.

For type 2 diabetes, based on models (1.2) and (1.3), we have $G_1 > G_2$. Generally we assume that $G_1 > G_{TH}$ and $G_2 < G^{TH}$. Then according to relationships among G_1, G_2, the lower threshold value G_{TH} and the upper threshold value G^{TH}, we have the following possible cases:

Case 1: $G_2 < G_{TH} < G^{TH} < G_1$,

Case 2: $G_2 < G_{TH} < G_1 < G^{TH}$,

Case 3: $G_{TH} < G_2 < G_1 < G^{TH}$,

Case 4: $G_{TH} < G_2 < G^{TH} < G_1$.

For Case 1, we can easily see that both equilibria E_1 and E_2 are virtual (see Fig.5(b)). It is clear that virtual equilibria can never be actually

attained. For example, a trajectory starting, say, in S_2 never approaches a stable virtual equilibrium E_2 and reverts to the glucose infusion state as soon as it crosses the lower threshold G_{TH}, while a trajectory starting in S_1 never approaches a stable virtual equilibrium E_1 and reverts to the insulin injection state immediately when it crosses the upper threshold G^{TH}. Combining these two observations, we find that the system may switch between the glucose infusion state (1.2) and the insulin injection state (1.3) forever. Fix all parameter values as those listed in Table 1. Simple calculations give $G_1 = 130.32mg/dl$ and $G_2 = 39.18mg/dl$. Choosing $G_{TH} = 65mg/dl$ and $G^{TH} = 115mg/dl$ within the normal range, Fig.5(a) shows that, for the given threshold window, the blood glucose level fluctuates periodically during the whole medical process. The durations of insulin injections and glucose infusions are shown in Fig.5(c), which suggests that the durations of each insulin injection and glucose infusion are stabilized at fixed values and the stable duration of glucose infusion is larger than the duration of insulin injection. In particular, we can obtain how fast the blood glucose level rebounds to the upper threshold value G^{TH} for type 1 diabetes (see Appendix D).

In order to further show the effect of a threshold window on the durations or number of insulin injections and glucose infusions switches for Case 1, we consider the following different settings for threshold windows (as shown in Fig.6). First, we fixed the width of the threshold window such that $G^{TH} - G_{TH} = 30mg/dl$, and let the lower threshold value G_{TH} increase from 60 to $90mg/dl$, where $G_{TH} = 60 + 1.5(n-1)$ for $n = 1, 2, ..., 21$ (see Fig.6(a) and Fig.6(b)). For the same width of threshold window, it is interesting to note that as G_{TH} increases, the duration of glucose infusion decreases (Fig. 6(b)) while the duration of insulin injection increases (Fig.6(a)). This indicates that, for the same width of threshold window, the larger the lower threshold value G_{TH}, the more the time needed for the blood glucose level to fall down to the lower threshold and the less the time needed for the blood glucose level to rebound to the upper threshold. Secondly, we fixed the upper threshold value $G^{TH} = 120mg/dl$, and let the lower threshold value G_{TH} vary from 60 to $90mg/dl$ with $G_{TH} = 60 + 1.5(n-1)$ for $n = 1, 2, ..., 21$ (see Fig.6(c) and Fig.6(d)). It follows that, as G_{TH} increases (and consequently as the threshold window becomes narrower), it takes more time for the blood glucose level to fall down or rebound, as shown in Fig.6(c). Finally, we fixed the lower threshold value $G_{TH} = 60mg/dl$, and let the upper threshold value G^{TH} increase from 75 to $105mg/dl$ with $G^{TH} = 75 + 1.5(n-1)$ for $n = 1, 2, ..., 21$ (see Fig.6(e) and Fig.6(f)). It is seen that, as G^{TH} increases

(and consequently as the threshold window becomes wider), the duration of the insulin injection monotonically increases whilst the duration of the glucose infusion decreases, and it is observed that the blood glucose level took more and more time to come down.

It follows from Fig.6(a) and Fig.6(e) that, as the upper threshold G^{TH} increases, the duration of insulin injection monotonically increases. So an issue is arising whether there is a certain value of the upper threshold value G^{TH} above which the insulin injection state with a threshold window cannot maintain the periodical fluctuation of the blood glucose level. Thus, could the normal range of the blood glucose level be maintained by using insulin therapy? To answer this question, we focus our discussion on Cases $2-4$ below.

For Case 2, the equilibrium E_1 becomes a regular steady state, which is globally stable for system (1.2) only. It is interesting to examine for the whole systems (1.2) and (1.3) how the blood glucose level behaves. It follows from Fig.7(a) and Fig.7(b) that any trajectory initiating from region S_1 or S_2 approaches the regular equilibrium E_1 for $G_{TH} = 65mg/dl$ and $G^{TH} = 140mg/dl$. It indicates that for a patient with an upper threshold for stopping injecting insulin, it may result in a constant blood glucose level without insulin therapy, which is dangerous for diabetes patients. For Case 3, we have that both equilibria E_1 and E_2 are regular and globally stable for their own systems. Fig.7(c) and Fig.7(d) show that the blood glucose level will approach certain levels represented by the equilibria E_1 and E_2, corresponding to a continuous treatment strategy (the insulin injection state) and free from insulin therapy (the glucose infusion state), under thresholds $G_{TH} = 30mg/dl$ and $G^{TH} = 140mg/dl$ (details see Fig.7(c) and Fig.7(d)). This suggests that the blood glucose level may be maintained at different fixed levels depending on the patient's initial blood glucose level. For Case 4, we have the virtual equilibrium E_1 and the regular equilibrium E_2, which is globally stable for system (1.3) only. Similarly to Case 2, the blood glucose level approaches a certain value corresponding to the insulin therapy, as shown in Fig. 7(e) and Fig.7(f).

4. Conclusion

Since the pioneering work on the dynamics of plasma insulin concentrations that led to the glucose-insulin regulatory system contributing to

insulin therapies, a number of research papers have appeared on the topic [2, 3, 10, 13, 15, 16, 39, 40]. Numerous studies have focused on the glucose-insulin regulatory system via a mathematical model of delay differential equations. Recently, Huang et al. proposed two novel mathematical models with impulsive injections of insulin or its analogues for type 1 and type 2 diabetes mellitus [13], and similar impulsive differential equations have been widely used in integrated pest management [28, 29, 41, 42]. In their paper, Huang et al. assumed that the constant glucose infusion rate G_{in} is described by a continuous process and insulin is injected once the blood glucose level reaches a threshold or at a fixed time. However, in clinical insulin therapies, the most satisfactory treatment would be: if the blood glucose level falls below a critical threshold, then injection of insulin is not applied and the patients can take up glucose with constant rate G_{in}; if the blood glucose level increases and exceeds a critical threshold, then insulin is injected with dose σ automatically and the glucose infusions are suspended. This regime is worked as a closed-loop technique which is integrated with a glucose monitoring system. Therefore, in this paper, we proposed piecewise glucose-insulin dynamic models with threshold windows, which extended the dynamic model (1.1). Hence the models formulated here can better describe the effect of insulin therapy on the blood glucose level.

The dynamics of models (1.2) and (1.3) with a single threshold were investigated. In particular, the sufficient and necessary conditions for the globally stable regular equilibrium and pseudo-equilibrium are provided by using qualitative analysis techniques of non-smooth Filippov dynamic systems. Furthermore, sliding bifurcations with respect to boundary node bifurcations have been studied by employing theoretical and numerical techniques. The results indicate that when choosing the single threshold G_C as a control parameter, the concentrations of glucose and insulin always stabilize at a regular equilibrium or a pseudo-equilibrium. However, in insulin therapies, to prevent the risk of hyperglycaemia or hypoglycaemia, it is critical to choose a desirable threshold level (here G_C) such that all equilibria of each system such as system S_1 and system S_2 become virtual, and the pseudo-equilibrium which is lying in the sliding mode domain is globally stable, then the blood glucose level can be controlled at a prescribed level within the normal range.

In addition, the dynamical behaviour of models (1.2) and (1.3) for type 2 diabetes with a threshold window were investigated numerically (for type 1 diabetes, the results are similar so we omitted them). We have studied several different scenarios based on the relations between the thresholds

and equilibria using the proposed models (1.2) and (1.3). Our results show that the blood glucose level can either fluctuate around the two prescribed thresholds or stabilize at an equilibrium for the insulin injection or glucose infusion state. In particular, for a patient with a fixed blood glucose level at the treatment starting time, it requires insulin injection and glucose infusion switches in a treatment regime to maintain the blood glucose level within the normal range for choosing an appropriate threshold window (for example $65 - 115 mg/dl$, see Fig.5). In contrast, if the upper threshold value is larger or the lower threshold value is smaller than the lower value of a normal range which corresponds to Case 2, 3 and 4 in section 3, the threshold window cannot maintain the periodical fluctuation of the blood glucose level. This indicates that the blood glucose level will approach certain levels represented by the equilibrium E_1 or E_2, corresponding to a continuous treatment strategy (the insulin injection state) or free from insulin therapy (the glucose infusion state), both of which increase the risk of hyperglycaemia or hypoglycaemia. Furthermore, insulin therapy is needed for a patient with a relatively high blood glucose level, while glucose infusion is required to maintain the blood glucose level above a safe level. This further confirms that it is important to individualize the treatment strategy for different patients with different initial blood glucose levels. Moreover, we have also shown (see Fig.6) that the effects of the thresholds and the widths of the threshold windows on the durations of insulin injection states and glucose infusion states are complex. The duration of the insulin injection state is more sensitive to the variation of thresholds compared to that of the glucose infusion state, for details see Fig.6(a) and Fig.6(e).

Note that the insulin degradation rate is assumed to be proportional to the insulin concentration, but it is more realistic to assume that the insulin degradation rate obeys Michaelis-Menten kinetics [16]. Moreover, the effect of physical exercise on the dynamics of glucose and insulin has been investigated [43], thus it would be interesting to know how this might affect the dynamics if we included it in our proposed models. Consequently, we plan to address these topics with the aim of improving optimal strategies for the treatment of diabetes in the near future, studies that will be reported elsewhere.

Acknowledgements: This work was supported by the Fundamental Research Funds for the Central Universities (GK201305010, GK201401004), and by the National Natural Science Foundation of China (NSFC,11171199,

11371030, 11301320).

Appendix A: The proof of Theorem 2.3

Note that if $0 \leq G_C < G_2$, then E_1 becomes a virtual equilibrium for subsystem S_1 and the tangent point E_T^1 of S_1 is invisible. Furthermore, E_2 is a regular equilibrium for subsystem S_2 and the tangent point E_T^2 of S_2 is visible, which indicates that the pseudo-equilibrium E_P does not exist in this case. Moreover, from Lemma 2.1, E_1 and E_2 are both globally asymptotically stable. Besides, E_2 is completely to the right of the threshold line $G = G_C$, i.e. in the region S_2, see Fig.3(a). Now we prove the global stability of E_2 of Filippov system (2.3).

It is easy to see that any solution initiating from the tangent point E_T^2 does not meet the threshold line $G = G_C$ again due to the stability of E_2, which must tend to E_2. On the one hand, any trajectory starting from region S_2 which hits the sliding segment Σ_S will move to E_T^2 along the sliding domain and then tend to E_2. On the other hand, the solution initiating from region S_2 reaches the threshold line $G = G_C$ and above the tangent point E_T^1 will enter into the region S_1.

Furthermore, any solution initiating from region S_1 of Filippov system (2.3) will reach the threshold line $G = G_C$ in a finite time. The solutions which meet the Σ_S will move to E_T^2 and then tend to E_2. Clearly, any trajectory which reaches the threshold line $G = G_C$ and below the tangent point E_T^2 will enter into region S_2, and consequently tends to E_2. Therefore, all solutions in system (2.3) finally converge to E_2.

Now we show that $0 \leq G_C < G_2$ are necessary conditions for the stability of E_2 of Filippov system (2.3). It is obvious that $G_C < 0$ is impossible. If $G_C = G_2$, then this contradicts the definition of the regular equilibrium of Filippov system (2.3); if $G_C > G_2$, then E_2 becomes a virtual equilibrium, and then the pseudo-equilibrium E_P follows which is stable with respect to sliding mode according to Lemma 2.2. These results contradict the global stability of the equilibrium E_2 of Filippov system (2.3). So $0 \leq G_C < G_2$ must hold. This completes the proof.

Appendix B: The proof of Theorem 2.4

Note that if $G_2 \leq G_C \leq G_1$, then E_1 and E_2 both become virtual equilibria E_V^1 and E_V^2 for Filippov system (2.3), which indicates that there exists a stable pseudo-equilibrium E_P in the sliding domain for Filippov system

(2.3) from Lemma 2.2. Further, the tangent point E_T^1 of subsystem S_1 and the tangent point E_T^2 of subsystem S_2 are both invisible (Fig.4(a)). Now we prove the global stability of the pseudo-equilibrium E_P of Filippov system (2.3).

First, all trajectories starting from region S_1 and S_2 which meet the sliding domain Σ_S will tend to the pseudo-equilibrium E_P according to Lemma 2.2. Second, all other trajectories will finally reach the sliding domain Σ_S and converge to the pseudo-equilibrium E_P. Otherwise, there must be some solution initiating from region S_1 or S_2 tending to another equilibrium, a limit cycle or infinity. These results contradict the properties of vector fields and nonexistence of a limit cycle of region S_1 and S_2. Therefore, the pseudo-equilibrium E_P of Filippov system (2.3) is globally asymptotically stable.

Now we prove that $G_2 \leq G_C \leq G_1$ are necessary conditions for the stability of the pseudo-equilibrium E_P. We first prove $G_C \geq G_2$. Otherwise, the condition $G_C < G_2$ ensures the stability of the regular equilibrium E_2 of Filippov system (2.3). Next we show that $G_C \leq G_1$ must hold true. Otherwise, if $G_C > G_1$, then E_1 becomes a regular equilibrium, and consequently the pseudo-equilibrium E_P does not exist according to Lemma 2.2. This contradicts the global stability of the pseudo-equilibrium E_P. Thus we have $G_2 \leq G_C \leq G_1$ must hold. The proof is complete.

Appendix C: The proof of Theorem 2.5

If $G_C > G_1$, then E_1 becomes a regular equilibrium and E_2 is a virtual equilibrium. From Lemma 2.2, the pseudo-equilibrium E_P does not exist (Fig.4(c)). Further, part of the sliding domain Σ_S is down below the x-axis.

Therefore, to prove the globally asymptotically stable E_1 of Filippov system (2.3), we only need to show that all solutions initiating from region S_2 will meet the threshold line G_C and enter into region S_1. In fact, it is evident that all solutions starting from region S_2 meet the threshold line G_C and then enter into region S_1 according to the properties of vector fields S_2. Furthermore, all solutions initiating from region S_1 converge to the equilibrium E_1. Then E_1 of Filippov system (2.3) is globally asymptotically stable.

Now we show that $G_C > G_1$ must hold true. Otherwise, if $G_C \leq G_1$, then E_1 becomes a virtual equilibrium, and consequently the stable pseudo-equilibrium E_P exists or the stable E_2 exists. This contradicts the global

stability of the equilibrium E_1. This completes the proof.

Appendix D: The duration of the glucose infusion state

For type 1 diabetes, the duration of the glucose infusion state can be described as follows:

$$\begin{cases} \dfrac{dG(t)}{dt} = G_{in} - \sigma_2 G(t) - a\left(c + \dfrac{mI(t)}{n + I(t)}\right) G(t) + b, \\ \dfrac{dI(t)}{dt} = -dI(t), \end{cases} \quad \text{until} G \downarrow G_{TH}. \tag{4.1}$$

We assume that the first time the blood glucose level drops and reaches the lower threshold value G_{TH} is at time t_1, i.e., we have $T(t_1) = G_{TH}$. Note that the analytical solution of the second equation of the model (4.1) with initial values of $T(t_1)$ can be obtained by direct integration, i.e.,

$$I(t) = I(t_1)exp(-d(t - t_1)), \quad t \geq t_1.$$

Substituting $I(t_1)$ into the first equation of (4.1) for $I(t)$, then integrating the first equation of (4.1) yields

$$\begin{aligned} G(t) &= G(t_1)exp[-\xi(t - t_1)](\tfrac{n+I(t)}{n+I(t_1)})^{\frac{ak}{d}} \\ &+ (G_{in} + b)(n + I(t))^{\frac{ak}{d}} \int_{t_1}^{t} \tfrac{exp[-\xi(t-u)]}{(n+I(u))^{\frac{ak}{d}}} du, \end{aligned}$$

suppose the blood glucose level went to the upper threshold G^{TH} at time t_2, i.e., we have $T_{t_2} = G^{TH}$, then we have the following equation

$$\begin{aligned} G^{TH} &= G_{TH}exp[-\xi(t_2 - t_1)](\tfrac{n+I(t_2)}{n+I(t_1)})^{\frac{ak}{d}} \\ &+ (G_{in} + b)(n + I(t_2))^{\frac{ak}{d}} \int_{t_1}^{t_2} \tfrac{exp[-\xi(t_2-u)]}{(n+I(u))^{\frac{ak}{d}}} du \end{aligned}$$

and solving the above equation with respect to t_2 gives the time $t_2 - t_1$ of the blood glucose rebounding from the lower threshold G_{TH} to the upper threshold G^{TH}.

References

[1] Bergman RN, Finegood DT, Kahn SE. The evolution of beta-cell dysfunction and insulin resistance in type 2 diabetes. Eur. J. Clin. Invest. 2002; 32: 35-45.

[2] Li JX, Kuang Y. Systemically modeling the dynamics of plasma insulin in subcutaneous injection of insulin analogues for type 1 diabetes. Math. Biosci. Engrg. 2009; 6: 41-58.

[3] Li JX, Kuang Y. Analysis of a glucose-insulin regulatory model with time delays. SIAM J. Appl. Math. 2007; 67: 757-76.

[4] Tolic IM, Mosekilde E, Sturis J. Modeling the insulin-glucose feedback system: The significance of pulsatile insulin secretion. J. Theor. Biol. 2000; 207: 361-75.

[5] Topp B, Promislow K, Deveries G, Miura RM, Finegood DT. A Model of β-cell mass, insulin, and glucose kinetics: pathways to diabetes. J. Theor. Biol. 2000; 206: 605-19.

[6] Maahs DM, Horton LA, Chase HP. The use of insulin pumps in youth with type 1 diabetes. Diabetes Technol. The. 2010; 12: S59-S65.

[7] Bode BW. Insulin pump use in type 2 diabetes. Diabetes Technol. The. 2010; 12: S17-S21.

[8] Raskin P, Bode BW, Marks JB, et al. Continuous subcutaneous insulin infusion and multiple daily injection therapy are equally effective in type 2 diabetes. Diabetes Care. 2003; 26: 2598-603.

[9] Roszler J. Senior pumpers: Some seniors may benefit from pump therapy even more than young people do. Diabetes Forecast. 2002; 55: 37-40.

[10] Li JX, Johnson D. Mathematical models of subcutaneous injection of insulin analogues: A mini-review. Discrete Contin. Dyn. Syst. B. 2009; 12: 401-14.

[11] Steil GM, Hipszer B, Reifman J. Mathematical modeling research to support the development of automated insulin-delivery systems. J. Diabetes Sci. Technol. 2009; 3: 388-95.

[12] Steil GM, Hipszer B, Reifman J. Update on mathematical modeling research to support the development of automated insulin-delivery systems. J. Diabetes Sci. Technol. 2010; 4: 759-69.

[13] Huang MZ, LI JX, Song XY, Guo HJ. Modeling impulsive injections of insulin: Towards artificial pancreas. SIAM J. Appl. Math. 2012; 72: 1524-48.

[14] Kanderian SS, Weinzimer S, Voskanyan G, Steil GM. Identification of intraday metabolic profiles during closed-loop glucose control in individuals with type 1 diabetes. J. Diabetes Sci. Technol. 2009; 3; 1047-57.

[15] Wang HL, Li JX, Kuang Y. Mathematical modeling and qualitative analysis of insulin therapies. Math. Biosci. 2007; 210: 17-33.

[16] Wang HL, Li JX, Kuang Y. Enhanced modeling of the glucose-insulin system and its applications in insulin therapies. J. Biol. Dyn. 2009; 3: 22-38.

[17] Kang H, Han K, Choi MY. Mathematical model for glucose regulation in the whole-body system. Islets. 2012; 4: 84-93.

[18] Tang SY, Xiao YN, Wang N, Wu HL. Piecewise HIV virus dynamic model with $CD4^+$ T cell count-guided therapy: I. J. Theor. Biol. 2012; 308: 123-34.

[19] Bernardo MD, Budd CJ, Champneys AR, et al. Bifurcations in nonsmooth dynamical systems. SIAM Rev. 2008; 50: 629-701.

[20] Brogliato B. Nonsmooth Mechanics. NY: Springer-Verlag; 1999.

[21] Costa MIS. Harvesting induced fluctuations: insights from a threshold management policy. Math. Biosci. 2007; 205: 77-82.

[22] Costa MIS, Meza MEM. Application of a threshold policy in the management of multispecies fisheries and predator culling. IMA Math. Med. Biol. 2006; 23: 63-75.

[23] Costa MIS, Kaszkurewicz E, Bhaya A, Hsu L. Achieving global convergence to an equilibrium population in predator-prey systems by the use of a discontinuous harvesting policy. Ecol. Model. 2000; 128: 89-99.

[24] Dercole F, Gragnani A, Rinaldi S. Bifurcation analysis of piecewise smooth ecological models. Theor. Popul. Biol. 2007; 72: 197-213.

[25] Doole SH, Hogan SJ. A piecewise linear suspension bridge model: nonlinear dynamics and orbit continuation. Dyn. Stab. Syst. 1996; 11: 19-29.

[26] Kuznetsov YA, Rinaldi S, Gragnani A. One parameter bifurcations in planar Filippov systems. Internat. J. Bifur. Chaos. 2003; 13: 2157-88.

[27] Meza MEM, Bhaya A, Kaszkurewicz E. Threshold polices control for predator-prey systems using a control Liapunov function approach. Theor. Popul. Biol. 2005; 67: 273-84.

[28] Tang SY, Liang JH, Xiao YN, Cheke RA. Sliding bifurcations of Filippov two stage pest control models with economic thresholds. SIAM J. Appl. Math. 2012; 72: 1061-80.

[29] Tang SY, Liang JH. Global qualitative analysis of a non-smooth Gause predator-prey model with a refuge. Nonlinear Anal. TMA. 2013; 76: 165-80.

[30] Filippov AF. Differential Equations with Discontinuous Righthand Sides. Dordrecht: Kluwer Academic; 1988.

[31] Buzzi CA, Silva PR, Teixeira MA. A singular approach to discontinuous vector fields on the plane. J. Differ. Equations. 2006; 231: 633-55.

[32] Buzzi CA, Carvalho TD, Silva PR. Canard cycles and Poincaré index of non-smooth vector fields on the plane. arXiv:1002.4169. 2010.

[33] Utkin VI, Guldner J, Shi JX. Sliding Mode Control in Electro-Mechanical Systems, seconded. Britain: Taylor and Francis Group; 2009.

[34] Li JX, Kuang Y, Mason C. Modeling the glucose-insulin regulatory system and ultradian insulin secretory oscillations with two time delays. J. Theor. Biol. 2006; 242: 722-35.

[35] Sturis J, Polonsky KS, Mosekilde E, Van Cauter E. Computer model for mechanisms underlying ultradian oscillations of insulin and glucose. Am. J. Physiol. 1991; 260: E801-E809.

[36] Gaetano AD, Arino O. Mathematical modeling of the intravenous glucose tolerance test. J. Math. Biol. 2000; 40: 136-68.

[37] Palumbo P, Panunzi S, Gaetano AD. Qualitative behavior of a family of delay differential models of the glucose-insulin system. Discrete Contin. Dynam. Syst. B. 2007; 7: 399-424.

[38] Palumbo P, Panunzi S, Gaetano AD. A discrete single delay model for the intra-venous glucose tolerance test. Theoret. Biol. Med. Model. 2007; 4: 35.

[39] Bolie VW. Coefficients of normal blood glucose regulation. J. Appl. Physiol. 1961; 16: 783-88.

[40] Nucci G, Cobelli C. Models of subcutaneous insulin kinetics: A critical review. Computer Methods and Programs in Biomedicine. 2000; 62: 249-57.

[41] Tang SY, Tang GY, Cheke RA. Optimum timing for integrated pest management: modeling rates of pesticide application and natural enemy releases. J. Theor. Biol. 2010; 264: 623-38.

[42] Tang SY, Liang JH, Tan YS, Cheke RA. Threshold conditions for interated pest management models with pesticides that have residual effects. J. Math. Biol. 2013; 66: 1-35.

[43] Derouich M, Boutayeb A. The effect of physical exercise on the dynamics of glucose and insulin. Journal of Biomechanics. 2002; 35: 911-17.

Table 1: Parameter values of models (1.2) and (1.3) for type 1 and type 2 diabetes.

Parameters	Values	Units	Parameters	Values	Units
σ_1	1.27	μ U/min	σ_2	5×10^{-6}	min^{-1}
a	0.02	mg^{-1}	b	85	mg/min
c	40	mg/min	d	0.08	min^{-1}
m	500	mg/min	n	80	mg
α_1	350	mg	G_{in}	50	mg/min
σ	1	U	$G_{TH}(G^{TH})$	60-120	mg/dl

Figure Legends

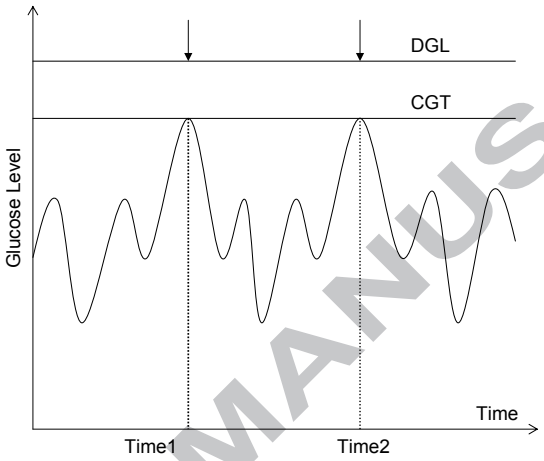

Figure 1: Dangerous glucose level (DGL)=lowest blood level that will cause harm to patients. Critical glucose threshold (CGT)= blood glucose level at which insulin should be injected to prevent an increasing blood glucose concentration from reaching the dangerous glucose level for patients. The arrows indicate points when the blood glucose levels exceed the critical glucose threshold and an insulin therapy method would be applied.

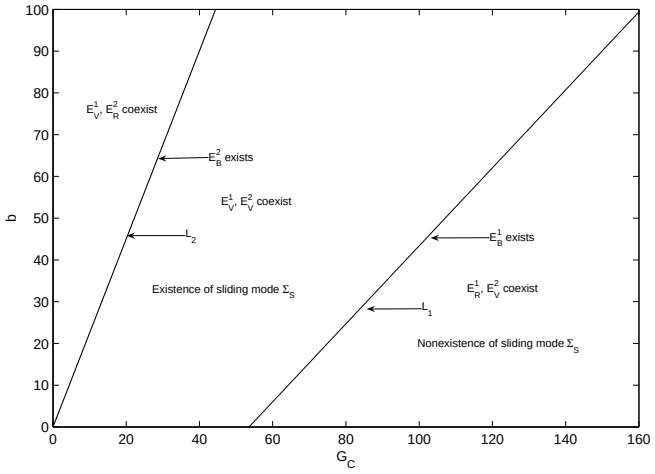

Figure 2: Bifurcation set of Filippov system (2.3) for type 2 diabetes with respect to b and G_C.

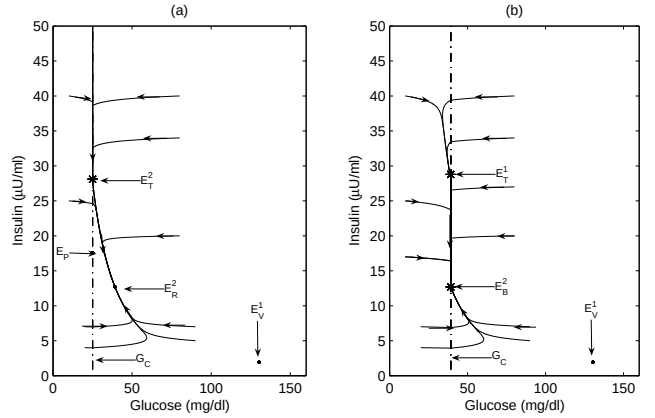

Figure 3: Boundary node bifurcation of Filippov system (2.3) for type 2 diabetes. (a) $G_C = 25mg/dl$; (b) $G_C = 39.18mg/dl$.

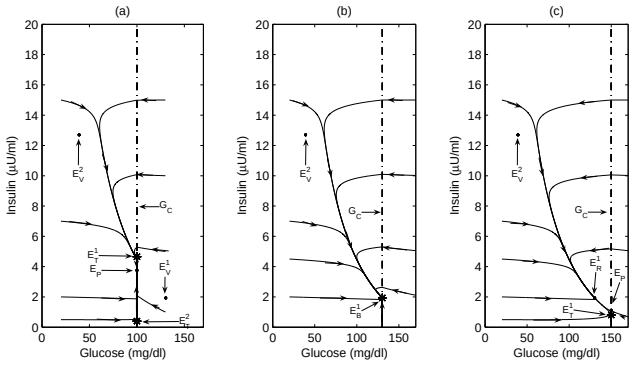

Figure 4: Boundary node bifurcation of Filippov system (2.3) for type 2 diabetes. (a) $G_C = 100mg/dl$; (b) $G_C = 130.32mg/dl$; (c) $G_C = 150mg/dl$.

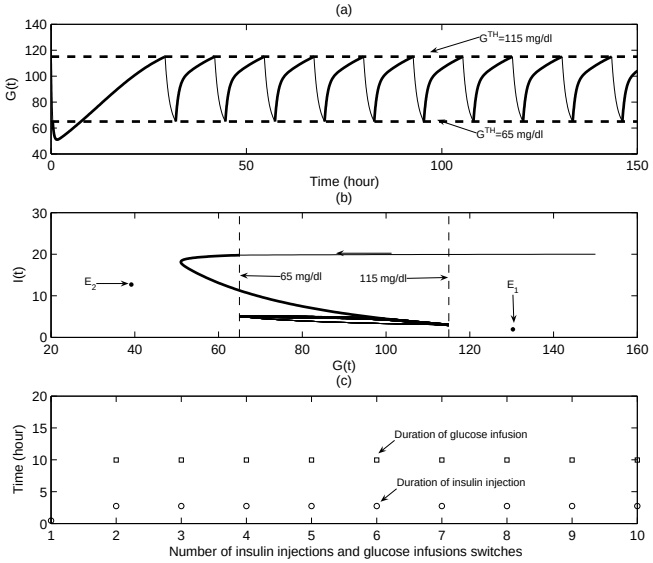

Figure 5: A simulation of typical solution of systems (1.2) and (1.3) for type 2 diabetes with $G_{TH} = 65mg/dl$ and $G^{TH} = 115mg/dl$ for Case 1. (a) Time series of the blood glucose level; (b) Phase plane plot of glucose and insulin concentrations; (c) Durations of insulin injection and glucose infusion for each switch.

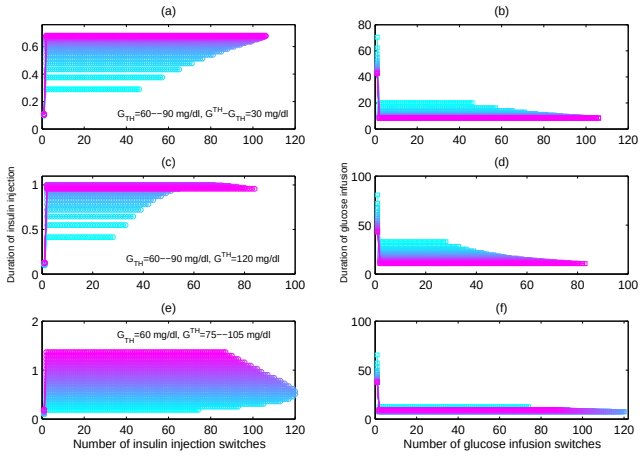

Figure 6: The effects of width of threshold window on the durations of insulin injection (or glucose infusion) and number of insulin injection and glucose infusion switches of systems (1.2) and (1.3) for type 2 diabetes. (a, b) We fixed the width of threshold window, i.e., let $G^{TH} - G_{TH}$ be a constant as $30mg/dl$, and G_{TH} increases from 60 to $90mg/dl$; (c, d) We fixed the upper threshold value G^{TH} as $120mg/dl$ and let the lower threshold value G_{TH} vary from 60 to $90mg/dl$; (e, f) We fixed the lower threshold value G_{TH} as $60mg/dl$ and let the upper threshold value G^{TH} increases from 75 to $105mg/dl$.

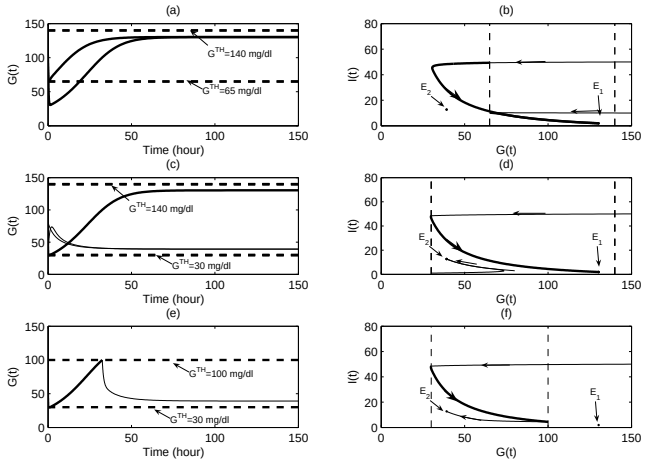

Figure 7: Numerical simulations of solutions of systems (1.2) and (1.3) for type 2 diabetes with different lower and upper threshold values. For Case 2: (a, b) Time series of the blood glucose level and phase plane plot of glucose and insulin concentrations with $G_{TH} = 65mg/dl$ and $G^{TH} = 140mg/dl$; For Case 3: (c, d) Time series of the blood glucose level and phase plane plot of glucose and insulin concentrations with $G_{TH} = 30mg/dl$ and $G^{TH} = 140mg/dl$: (e, f) Time series of the blood glucose level and phase plane plot of glucose and insulin concentrations with $G_{TH} = 30mg/dl$ and $G^{TH} = 100mg/dl$.

1. We develop novel piecewise glucose-insulin models with a threshold window for diabetes mellitus.

2. Bifurcation analysis and clinical outcomes are addressed for the proposed models with a single threshold.

3. The effects of thresholds on the durations of insulin injection and glucose infusion are investigated.

4. The blood concentrations of patients can be maintained within a normal range using the proposed models.

5. The desirable thresholds must be chosen carefully and insulin therapy must be individualized for each patient.